Polystyrene-Coated Alumina Powder Via Dispersion Polymerization for Indirect Selective Laser Sintering Applications

Ludwig Cardon,[1,2] Jan Deckers,[3] An Verberckmoes,[1] Kim Ragaert,[1,2] Laurens Delva,[1,2] Khuram Shahzad,[4] Jef Vleugels,[4] Jean-Pierre Kruth[3]

[1]Center for Polymer and Material Technologies CPMT, Associated Faculty of Applied Engineering Sciences, University College Ghent, Voskenslaan 362, 9000 Ghent, Belgium
[2]Associated Faculty of Materials Science and Engineering, Ghent University, Technologiepark 903, B-9052 Ghent, Belgium
[3]Division PMA, Department of Mechanical Engineering, Katholieke Universiteit Leuven, Celestijnenlaan 300B, B-3001 Heverlee, Belgium
[4]Department of Metallurgy and Materials Engineering, Katholieke Universiteit Leuven, Kasteelpark Arenberg 44, B-3001 Heverlee, Belgium
Correspondence to: L. Cardon (E-mail: Ludwig.Cardon@ugent.be)

ABSTRACT: A promising method for the manufacture of complex 3D ceramic parts is selective laser sintering (SLS). SLS of alumina components can be done either directly or indirectly. In this article, the indirect method is used by using polystyrene coated alumina particles. One of the methods to produce these alumina powders is dispersion polymerization. In this research, it is described how the alumina powder has been developed and tested. The powder has been characterized to define its processability within the SLS process. Used techniques include SEM (morphology), STA/TGA (overall mass loss), DSC (glass transition temperature T_g), and laser diffraction (particle size distribution). The investigated SLS process parameters were the preheating temperature, laser power, scan spacing, and scan speed. STA/TGA has proven that polystyrene-coated alumina powders are suitable for SLS process, while DSC results were judged to be a good source of complementary data on preheating temperature of alumina/polystyrene powders. SLS experiments showed that single layer green parts can be produced. By using the optimized SLS parameters, it was demonstrated that different 3D geometries can be produced with the polystyrene coated alumina powders. © 2012 Wiley Periodicals, Inc. J. Appl. Polym. Sci. 000: 000–000, 2012

INTRODUCTION

Polymer-coated inorganic particles have demonstrated interesting properties in areas such as adhesives, textiles, optics, electronics, and controlled release.[1–3] A promising application of ceramic powders coated with an organic binder is indirect selective laser sintering (SLS).[4–7] SLS is a powder-based additive manufacturing (AM) process to fabricate complex shaped parts.[8,9] It is one of the few rapid prototyping (RP) methods that can shorten the design manufacturing cycle and can produce parts directly from powders. The SLS process, illustrated in Figure 1, is using a roller system to deposit successive layers of powder. The starting powder should be free-flowing and therefore spherical shaped powders are preferred.[10] A laser beam is used as heating source for selectively sintering each powder layer according to predefined geometries by partially melting the powder particles.

To overcome the problem of porous and fragile parts[11–13] colloidal processing based techniques[14–16] and selective laser melting (SLM)[17] are known to produce high density layers and parts.

Different suitable polymeric and metal powders are commercially developed for the production of functional parts via SLS processing.[8,18] Zheng investigated the sintering behavior and mechanical properties of alumina nanoparticles coated with styrene by emulsion polymerization.[7] Chemical modification of alumina through grafting can create strong interfacial interaction between alumina and PS upon emulsion polymerization.[19] Core-shell SiO_2/PS nanocomposite particles were synthesized through mini-emulsion polymerization by using sodium lauryl sulfate surfactant,[20] or by

1 CO₂ leaser beam
2 Optics
3 Scanning mirrors
4 Thin Layer of powder
5 Powder levelling roller
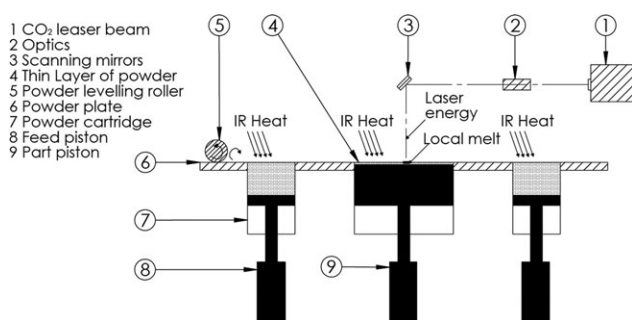6 Powder plate
7 Powder cartridge
8 Feed piston
9 Part piston

Figure 1. The selective laser sintering process.

first grafting with oleic acid followed by *in situ* emulsion polymerization with sodium dodecyl sulfonate surfactant.[21] The disadvantage of emulsion polymerization is however that emulsifiers often pollute the core-shell type composites and negatively impact their smoothness and morphology.[22] Such disadvantages can be overcome through dispersion polymerization that does not use emulsifiers.[23–26] A continuous and dense polymer layer coating was demonstrated in the case of polystyrene coating of Fe_3O_4 particles using dispersion polymerization.[27] A novel phase inversion technique using DMSO as solvent was applied to produce homogeneous Al_2O_3/PA composites, however with modest green and sintered densities of the parts.[6]

SLS of alumina components can be done directly or indirectly. The indirect approach applied in this work uses polymer-coated alumina particles and a two step process. In a first step, the polymer coating is selectively melted with a laser beam through layer by layer scanning. This results in melting of a polymeric binder phase to produce the so called "green parts," illustrated in Figure 2. After the laser sintering step, the binder phase is removed and the density of the part is improved by furnace sintering and/or infiltration. Direct selective laser sintering does not involve a sacrificial binder phase and the material is directly sintered or melted to produce parts.[10]

In this article, we report the study of the development and SLS sintering behavior of polystyrene-coated alumina particles using dispersion polymerization. We investigated the effect of the synthesis conditions and the percentage of polystyrene (%PS) coating on the flowability of the powders and on the sintering performance at varying process parameters including scan speed, scan spacing and laser power for a single layer. Thermogravimetric analysis (TGA) is often used to determine weight loss of a material over a certain interval of time or temperature.[28–31] Within this research, TGA analysis provides a good indication of the percentage of polystyrene binder coating. Additional characterization via differential scanning calorimetry (DSC) is also performed. From the DSC analysis the glass transition temperature T_g and the SLS heating conditions could be defined. Illustrations are provided of the production of 3D parts with different shape.

EXPERIMENTAL

Materials
The purity and sources of the chemicals were: styrene (99.5%, Acros Organics), divinylbenzene (DVB) (stabilized with 4-tert-butylpyrocatechol, Merck), 2,2-azobisisobutyronitrile (AIBN)

(98%, Acros Organics), ethanol (99.9%, Merck). High purity α-alumina (grade SM8, Baikowski, France) powder with a D50 ∼0.3 μm was used as structural material.

Dispersion Polymerization and Powder Production
A batch of material was prepared in a 500-mL three-neck flask equipped with a thermometer and a reflux condenser. The flask was covered with aluminum foil and immersed in a water bath that was placed on a heating plate with magnetic stirrer capacity. A mixture of 283.5 g ethanol and 16.5 g water was heated to above 50°C and 55.58 g styrene, 0.58 g divinylbenzene (DVB), and 30.11 g alumina were poured into the solution and stirred with magnetic stirrer agitation. The mixture was heated to 65°C and finally 0.565 g azobisisobutyronitrile (AIBN) was added. The dispersion polymerization was carried out at 65°C for 6.5 h upon magnetic stirring. After reaction, the final product was cooled down to room temperature. The next day the mixture was filtered and three times washed with water. The solid product was dried in an oven at 50°C for 2 h to remove all solvents. After the drying process, the material prepared in the 500-mL flask was divided in two parts. A first part of the material was manually crushed in a mortar. A second part of the material was grinded in a ball-mill (Fritsch 500-111) to obtain fine powder. This powder was afterwards sieved (Retsch AS200 digit) with a mesh size sieve of 160 μm. In a second test, the above 500-mL recipe was scaled up to a 2-L recipe in a 3-L four-neck flask by multiplying the amounts of each of the individual ingredients by four, using 1134 g ethanol, 66 g water, 222.32 g styrene, 2.32 g divinylbenzene, and 120.44 g α-alumina powder and 2.26 g 2,2-azobisisobutyronitrile. The preparation was similar and the polymerization was executed at a temperature of 65–67°C for 6.5 h upon magnetic stirring. The powder prepared in the 3-L flask was grinded in a ball-mill followed by sieving with a mesh size sieve of 160 μm. This powder was used in the single layer SLS tests. Finally, for the production of the powder for 3D layer SLS tests, the 2000 mL preparations were repeated to produce a large batch of powder. This larger powder batch was ball-milled, followed by sieving with a mesh size sieve of 125 μm. The reduction of the mesh size was chosen because the 125 μm corresponds to half the layer size in SLS.

STA/DSC Analysis
The STA analysis of the developed PS-coated alumina powder is done using Netzsch 449 F3 Jupiter STA equipment under
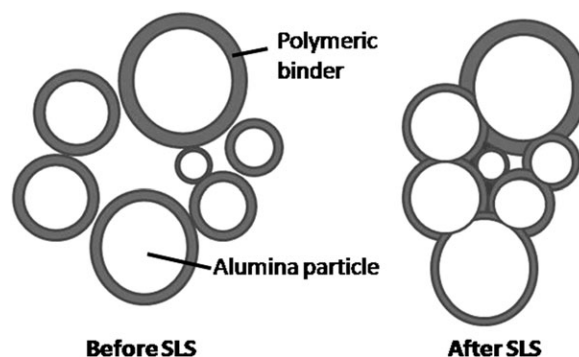

Figure 2. Schematic presentation of powder before and after SLS process.

protective nitrogen atmosphere measuring combined TGA and DSC. Samples were heated to 1500°C at a heating rate of 10°C min^{-1}. Mass change (%) was determined via Netzsch Proteus TA software providing the wt % PS coated on the Al_2O_3 particles.

Differential scanning calorimetry (DSC) was performed using a Netzsch 204 F1 equipment under nitrogen atmosphere. Approximately 25 mg of sample material in an open aluminum pan was referenced against an empty open aluminum pan. Samples were heated to 150°C at a heating rate of 10°C min^{-1}. Netzsch Proteus TA software was used to determine T_g.

Digital Microscopy/SEM
Digital microscope pictures of manually crushed and ball milled powder after powder production and samples after burning out the polymer within the STA equipment were taken using a Digital Microscope VHX-500 F from Keyence. Scan electron microscopy analysis of the powder after laser scanning in the SLS station was performed on a scanning electron microscope (SEM type: XL 30 FEG, Philips, The Netherlands).

Particle Size Distribution
Particle size distribution measurements were performed using a Laser Diffraction particle size analyzer (Malvern Mastersizer-S, long bench, Malvern Instruments, Malvern, UK). The polymer coated alumina particles were dispersed in miglyol to obtain well dispersed powder particles for the measurement.

Indirect Selective Laser Sintering Tests
Indirect selective laser sintering tests were performed with a DTM Sinterstation 2000 (DTM Corporation/3D Systems, USA) equipped with a 100 W CO_2 laser (f100, Synrad, USA) with a wavelength of 10.6 μm and a laser beam diameter of 400 μm. Single layer tests were performed with the 160-μm sieved PS-coated alumina particles (2-L recipe). The powder was preheated to ∼ 90°C, which is ∼ 20°C lower than the glass transition temperature T_g of PS. The energy required to melt PS was partly supplied by preheating of the powder bed to a temperature below T_g and partly by laser irradiation to a temperature above T_g. The 125 μm sieved PS-coated alumina particles are used in the production of 3D parts with SLS. The 3D parts were produced with a layer thickness of 250 μm and with the following optimized parameters: laser power of 17 W, scan speed of 900 mms^{-1}, scan spacing of 0.1 mm.

RESULTS AND DISCUSSION

Dispersion Polymerization
In dispersion polymerization the monomer and the initiator are both soluble in the polymerization medium, but the medium is a poor solvent for the resulting polymer. The polymerization is initiated in a homogeneous solution, but depending on the solvency of the medium for the resulting macromolecules, phase separation occurs.[32] Most often a stabilizer is added [e.g., poly-vinylpyrrolidone,[27] poly(acrylic acid)],[26,33] which can have the disadvantage to form very stable dispersions that cannot be filtered. Instead we avoided the use of a dispersion stabilizer to form agglomerates that are easily filtered out. For the coating process the presence of the divinyl benzene as crosslinking reagent is crucial. The vinyl groups of the DVB crosslinking rea-
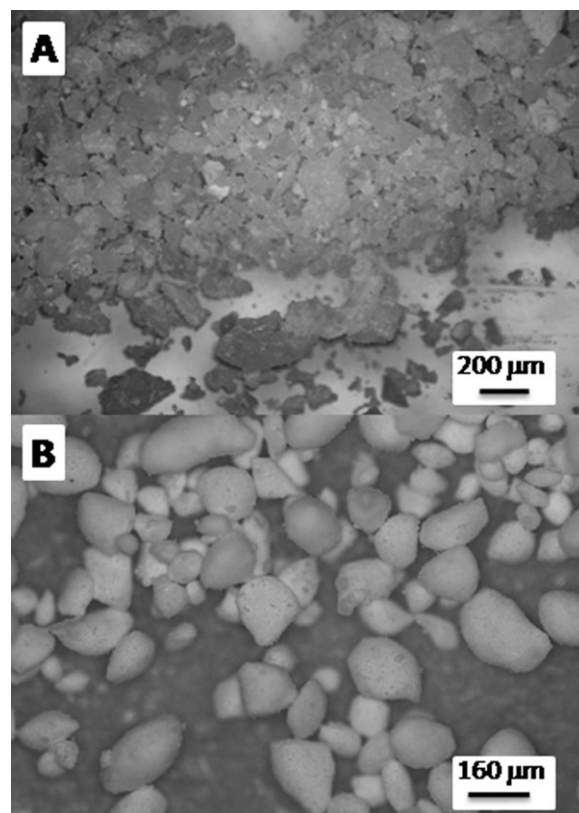

Figure 3. Digital microscope pictures of (A) Manually crushed Al_2O_3/30 wt %PS powder and (B) Ball-milled grinded and sieved powder with a mesh size sieve of 160 μm.

gent provide reactive C=C bonds capable of copolymerizing with styrene to form a dense polymer layer or binder coating around the inorganic alumina particles. The polymerization experiments were carried out in a dark reactor to avoid faster polymerization due to reaction with UV light that could afterward result in a bad distribution of the PS and ceramic material, resulting in a non homogeneous powder mixture and bad green parts during the sintering process. The initiator AIBN is added at the end to prevent premature polymerization and to only initiate the reaction when all composite ingredients are present at appropriate polymerization temperature.

Al_2O_3/PS Agglomerate Size and Shape
The initial organic alumina particles have a D50 of around 0.3 μm and the resulting polymer-coated Al_2O_3/PS agglomerates formed are processed by (a) crushing in a mortar or by (b) dry grinding in a ball-mill followed by sieving. Figure 3(A) illustrates microscope pictures of manually crushed powder. Figure 3(B) is the result of ball-mill grinded and sieved powder, with a sieve mesh size of 160 μm. A clear difference between the two powders can be noticed. The manually crushed powder is sharp-edged, while the ball-mill procedure results in particles that have a more round shape. As a consequence of the sieving, the materials in Figure 3(B) have in addition a more homogeneous particle size distribution. Upon dry grinding of powders in a ball-mill both breakage and agglomeration phenomena can take place.[34] Ball-milling of alumina/polyamide powder
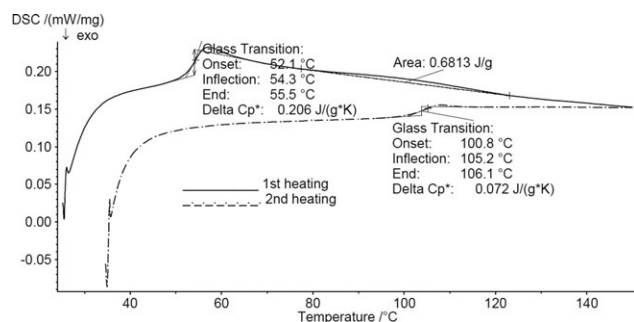
Figure 4. DSC result for 500 mL batch.

Figure 6. Side image of bound powder after STA analysis.

agglomerates has been reported earlier by Deckers et al. for the processing of high density technical ceramic parts through SLS.[35] Ball-milling was also applied in an SLS study of high-density alumina ceramic parts for mixing alumina powder with stearic acid in a ball-mill, however the average alumina particle size there was only 0.26 μm.[5]

DSC Results

DSC measurements are performed to study the thermal behavior, suitability, and processing behavior of polymers in the SLS process.[36,37] The result of the DSC test for the 500-mL batch is illustrated in Figure 4. The data of the Al_2O_3/30 wt % PS sample is collected to measure the glass transition temperature T_g. A two stage heating is applied. During the first heating cycle, the initial T_g of the PS during the synthesis is around 54°C. This implies short chain lengths and low average molecular weight of the PS initiated around the alumina particles, as the T_g is function of the average molecular chain length M_n.[38] A T_g of 54°C correlates with an average molecular chain length between 3000 and 4000 g mol^{-1}. A small endothermic peak of 0.68 J g^{-1} and the decreasing base line (decreasing heat capacity) indicate both the evaporation of unpolymerized styrene.

The second heating cycle shows an increase of the T_g to 104°C. This indicates the formation of a stable PS layer during the preheating phase at 90°C and the following laser sintering process. The temperature rise gives the polymer chains more flexibility and gives the possibility to the reactive end groups to further react as a living polymerization to a higher T_g than the preproduction step. This means the preproduction step as described in
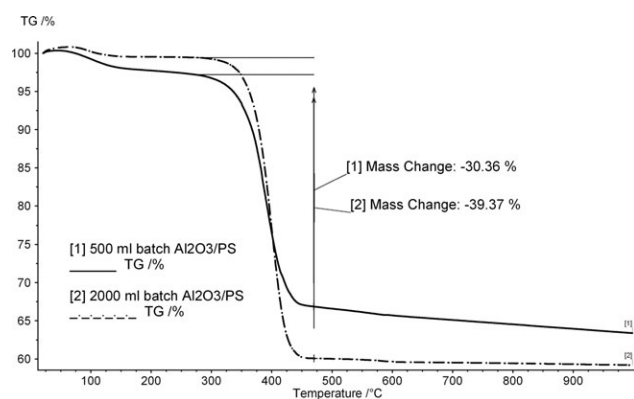
this article can be shortened. Concerning the 2-L batch, the same T_g has been detected. The observed value of 105°C is close to the reference value of 100°C for pure PS.[39,40] The increase of the T_g value can be related to the immobility of the polymer chain at the Al_2O_3 surface. Similarly, Haldorai et al. explained an elevated T_g value of 103°C for silica/polystyrene core-shell composites compared to a T_g value of 99.8°C measured for pure polystyrene by the immobility of polystyrene at the SiO_2 surface.[41] Besides, one must notice that a value of 105°C is well within the range of measured T_g values of polystyrene on different DSC-instruments as the T_g value depends on the thermal history of the sample, the heat flow and the sample size.[42]

STA Results

Results of the STA tests are illustrated in Figure 5. During the initial heating phase, some minor mass loss has already occurred, which can most likely be attributed to a drying effect of the raised temperature. The 500-mL batch sample has 1–2% more mass loss in the initial phase due to relative more evaporation of residual solvent (water, ethanol) and unpolymerized styrene. Around 400°C both curves show a mass loss due to the decomposition of the polystyrene at the depolymerization temperature and the mass loss values were calculated from the first derivative of the mass loss with temperature. TG showed that there is a weight loss of respectively, 30.36 and 39.37 wt % for the 500 mL and 2 L prepared Al_2O_3/PS batches. According to the STA results, the material of the 500 mL batch contained 30.36 wt % PS, denoted in this article as the Al_2O_3/30 wt %PS sample. STA results of the 2-L batch indicated that a material
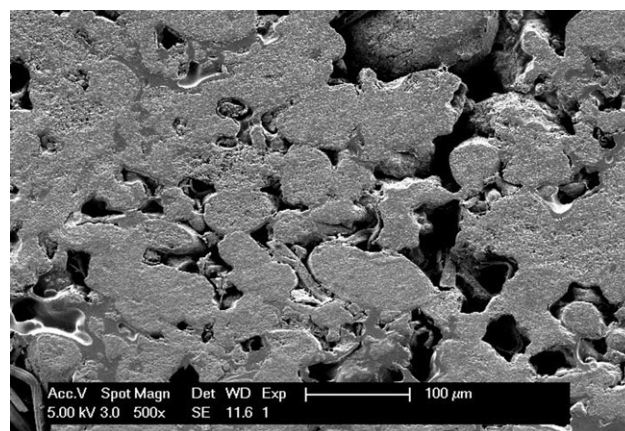

Figure 5. Mass loss as a result of extended heating.

Figure 7. SEM images of bound powder.

Table I. Sintering Tests with Batches Al$_2$O$_3$/30 wt % PS and Al$_2$O$_3$/39 wt % PS and with Variation of Scan Speed, Scan Spacing, and Laser Power

	Test 1	Test 2	Test 3
Al$_2$O$_3$/%PS	30	30	39
Scan speed (mm s^{-1})	500–1000	100–500	100–1000
Scan spacing (mm)	0.15–0.25	0.1–0.3	0.1–0.3
Laser power (W)	10	10	10
[O$_2$]	<5%	<5%	<5%
Thermocouple temperature (°C)	85–87	90–91	90–92
Sieving	N	Y	Y
Flowability	–	+	+
Stronger parts	–	–	+

Figure 9. Pores in the scanned powder.

with a higher wt % PS of 39.37 wt % was produced, denoted as Al$_2$O$_3$/39 wt %PS.

Sintering Results after STA

After burning out the polymer within the STA equipment, and after controlled cooling down of the sample, the powder remains bound. This is illustrated in Figure 6 for the Al$_2$O$_3$/30 wt % PS powder sample that was crushed in a mortar. The powder remains in the shape of the sample carrier and is relatively strong. Figure 7 is the SEM images of this powder after burning out of the polymer within the STA equipment. Because the burning temperature (1300°C) exceeds by far the sinter temperature, the powder is sintered, the polystyrene binder is burned out and neck formation has been established.

Indirect Sintering Tests: Single Layer Tests

In this article a first assessment of the green parts fabrication of Al$_2$O$_3$/PS ceramics by SLS is being investigated. The process parameters that were varied in this study are the laser power, the laser beam scan speed, and the laser beam scan spacing. The powder variables in this study are the particle size (distribution—manually crushed or ball milled) and amount of PS coated on the alumina. One layer of powder was scanned in the
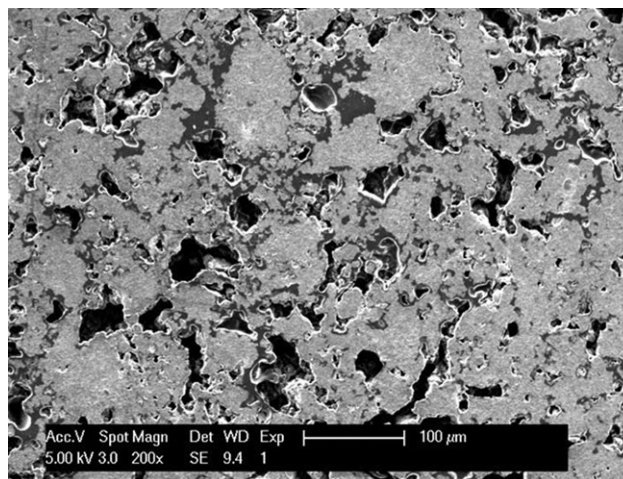
DTM Sinterstation 2000. The sintering parameters are listed in Table I.

In a first sintering test the batch Al$_2$O$_3$/30 wt %PS that was manually crushed in a mortar was evaluated. The flowability of the powder was not good and no strong connections were formed during the laser scanning. SEM analysis of the scanned powder shows neck formation (Figure 8) but also big pores (Figure 9). These pores are the result of the flow of the powder during the coating of the layer, which is not yet optimal. This is explained as the powder was developed by manually crushing and no sieving of the powder, so that a non uniform and non size controlled powder was applied.

For the second and third set of sintering tests the Al$_2$O$_3$/30 wt % PS and Al$_2$O$_3$/39 wt % PS powders were selected. Both powders were ball-milled and sieved to particles with a mesh size sieve of 160 μm. The tests allow to evaluate both the effect of the powder treatment (ball-milling and sieving) and the effect of the amount of polystyrene coating that forms the binder layer between the alumina particles, finally resulting in the green part.
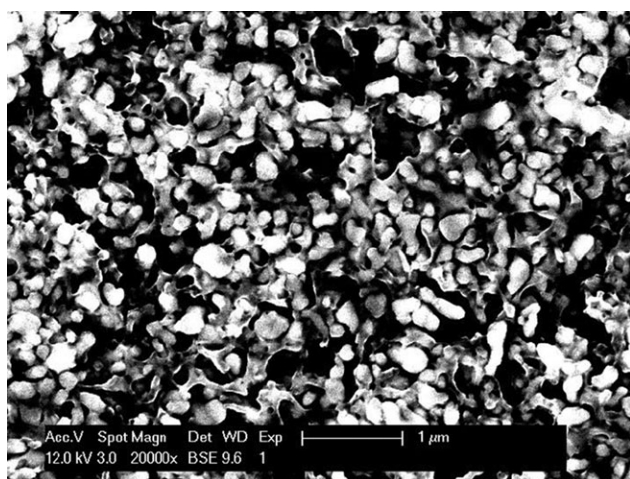

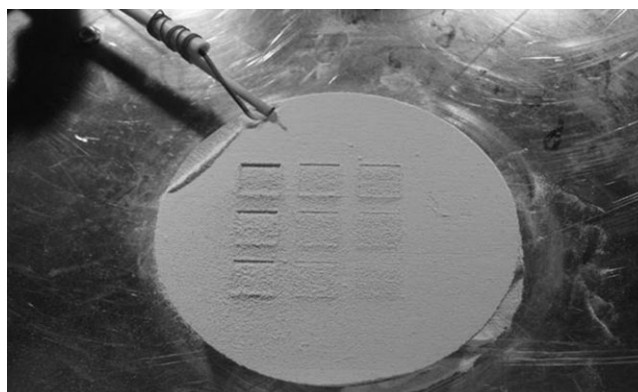**Figure 8.** Neck formation in the scanned powder.

Figure 10. Second single layer sintering test with the sieved Al$_2$O$_3$/30 wt %PS ceramic powder. The dimensions of the squares are 15 × 15 mm^2.
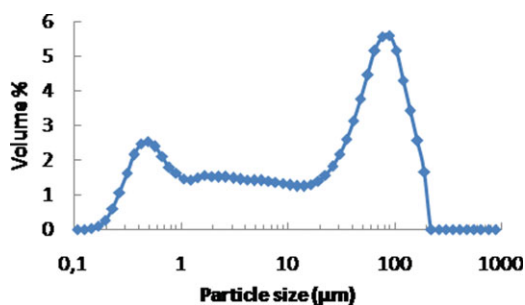
Figure 11. Particle size distribution of the larger scale production of sieved powder with a mesh size sieve of 125 μm. [Color figure can be viewed in the online issue, which is available at wileyonlinelibrary.com.]

All samples produced in the second test, using the sieved Al_2O_3/30 wt % PS powder, were laser sintered with a lower scan speed, while a broader range of scan spacing was tested and the pre-heating temperature was slightly higher compared to the first sintering test (Table I). The sieved powder showed a very good flowability. Figure 10 presents the second sintering test and illustrates the good flowability of the powder that forms a smooth, thin continuous layer.

Although the flowability of the Al_2O_3/30 wt % PS powder is very good, the sintering tests did not result in strong
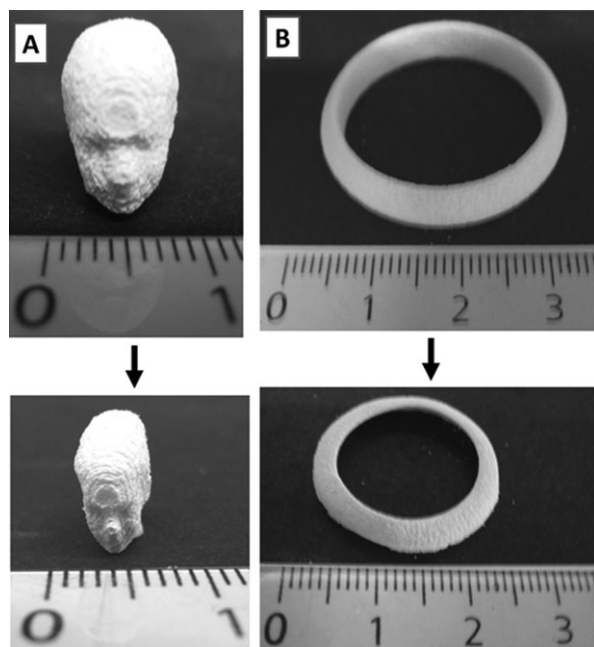

Figure 12. Small test parts in the shape of a head (A) and ring (B) before (top) and after (bottom) debinding and sintering.
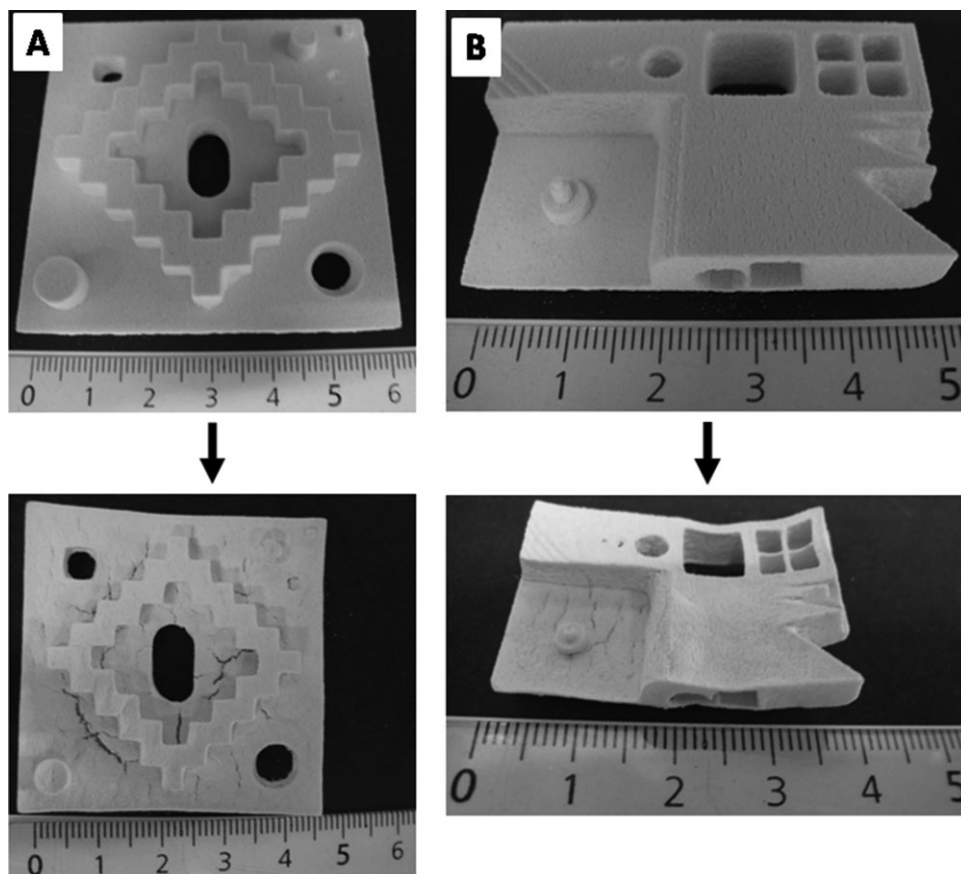

Figure 13. Large geometrical test parts (A, B) before (top) and after (bottom) debinding and sintering.

connections during single layer tests, with variation of the parameters as shown in Table I.

In a third sintering test the Al_2O_3/39 wt % PS powder with 39 wt % polystyrene coating was tested with a broad scan spacing (0.1–0.3 mm) and scan speed range (100–1000 mms^{-1}) and finally strong connections were made during the laser scanning. Thus the increased amount of polystyrene caused improved green strength and the ball-milling and sieving was necessary to improve the flowability.

3D Parts Production with SLS

After the promising single layer tests, more material was produced by repeating several 2-L recipes (always mechanically stirred and with stabilized polymerization temperature) to perform multilayer 3D sintering tests for the formation of the green parts and analyzing the green and postsintered densities. To improve the flowability of the powder, sieves with mesh size of 125 μm instead of 160 μm were used, which is half of the layer thickness of the "fixed" SLS process layer parameter of 250 μm. The PSD is shown in Figure 11. The D10, D50, and D90 values are respectively, 0.5, 25, and 110 μm.

The SLS parameters were optimized based on a parametric study that was executed with 18 cubic parts of 10 × 10 × 10 mm^3, and the optimized parameters were a laser power of 17 W, scan speed of 900 mms^{-1} and scan spacing of 0.1 mm.[43] Small parts in the shape of a head and a ring were produced as illustrated in Figure 12. These small parts did not give surface cracks. The green parts do shrink upon debinding and solid state sintering (bottom figures). Also larger geometrical test parts were produced (Figure 13), but these parts contain large surface cracks after the debinding and sintering step and show curling.

Ongoing Improvements on the Powder Production

Compared with conventional PS production, the amount of AIBN initiator will be optimized. The AIBN concentration affects the styrene conversion and relative molecular weights.[44] It is expected that the AIBN concentration influences the T_g value of PS coating, resulting in better flowability of the alumina/PS powder at high temperatures and better sintering conditions. Also the concentration of DVB and addition time of the cross-linking reagent can be optimized.[45] Furthermore, the reaction time of the dispersion polymerization will be lowered to optimize the process. Actually, this powder optimization research is going on.

CONCLUSIONS AND OUTLOOK

The present work confirmed that it is possible to produce alumina parts through selective laser sintering (SLS) and proper powder production via dispersion polymerization of alumina coated with PS. The dispersion polymerization is performed without dispersion stabilizer in a water–ethanol mixture using divinylbenzene as crosslinking reagent and AIBN as initiator. About 500 and 2000 mL batches of polymer-coated alumina particles were prepared, containing respectively, 30 and 39 wt % PS on alumina. The powder has been characterized to define its processability within the SLS process. Used techniques include SEM, STA/TGA, and DSC. The investigated SLS process param-

eters were the preheating temperature, laser power, scan spacing, and scan speed. STA/TGA has proven that polystyrene coated alumina powders are suitable for SLS process, while DSC results were judged to be a good source of complementary data on preheating temperature of alumina/polystyrene powders. From the indirect sintering tests and green parts fabrication some conclusions can be made. First, to obtain a good flowability it is better to ball-mill and sieve the dried powders than to manually crush them in a mortar. Ball-milling and sieving is necessary to get round shaped PS-coated alumina particles with a controlled particle size and distribution. Second, to obtain stronger green parts only the highest amount of %PS at the coating was successful. Finally, it was demonstrated that different 3D geometries can be produced with the PS-coated alumina powders, but only the smallest parts did not contain cracks.

REFERENCES

1. Haga, Y.; Inoue, S.; Sato, T.; Yosomiya, R. *Angew. Makromol. Chem.* **1986,** *139,* 49.

2. Creatura, J. A.; Hsu, G. R. US Patent 4,937,166, 1990.

3. Scarfato, P.; Russo, P.; Acierno, D. *J. Appl. Polym. Sci.* **2011,** *122,* 3694.

4. Subramanian, K.; Vail, N.; Barlow, J.; Marcus, H. *Rapid Prototyping J.* **1995,** *1,* 24.

5. Liu, Z.; Nolte, J.; Packard, J.; Hilmas, G.; Dogan, F.; Leu, M. *Proc. 35th Int. Matador Conf.* **2007,** *14,* 351.

6. Shahzad, K.; Deckers, J.; Boury, S.; Neirinck, B.; Kruth, J.-P.; Vleugels, J. *Ceram. Int.* **2012,** *38,* 1241.

7. Zheng, H.; Zhang, J.; Lu, S.; Wang, G.; Xu, Z. *Mater. Lett.* **2006,** *60,* 1219.

8. Kruth, J.-P.; Levy, G.; Klocke, F.; Childs, T. H. C. *CIRP Ann. Manufact. Technol.* **2007,** *56,* 730.

9. Kumar, S. *J. Miner. Metals Mater. Soc.* **2003,** *55,* 43.

10. Dickens, J. E. D.; Lee, B. L.; Taylor, G. A.; Magistro, A. J.; Ng, H.; McAlea, K. P.; Forderhase, P. F. US Patent RE39,354, 2006.

11. Kolosov, S.; Vansteenkiste, G.; Boudeau, N.; Gelin, J. C.; Boillat, E. *J. Mater. Process. Technol.* **2006,** *177,* 348.

12. Rahaman, M. N. Ceramic Processing and Sintering; Marcel Dekker: New York, **1995.**

13. Bertrand, P.; Bayle, F.; Combe, C.; Goeuriot, P.; Smurov, I. *Appl. Surf. Sci.* **2007,** *254,* 989.

14. Klocke, F.; Derichs, C.; Ader, C.; Demmer, A. *Prod. Eng. Res. Dev.* **2007,** *1,* 279.

Applied Polymer
JOURNAL OF
SCIENCE

15. Wu, Y.; Du, J.; Choy, K.-L.; Hench, L. L. *J. Eur. Ceram. Soc.* **2007,** *27,* 4727.

16. Gahler, A.; Heinrich, J. G. *J. Am. Ceram. Soc.* **2006,** *89,* 3076.

17. Hagedorn, Y.-C.; Wilkes, J.; Meiners, W.; Wissenbach, K.; Poprawe, R. *Phys. Proc.* **2010,** *5,* 587.

18. Dewidar, M. M.; Lim, J.-K.; Dalgarno, K. W. *J. Mater. Sci. Technol.* **2008,** *24,* 227.

19. Zeng, Z.; Yu, J.; Guo, Z. X. *Macromol. Chem. Phys.* **2005,** *206,* 1558.

20. Zhang, S. W.; Zhou, S. X.; Weng, Y. M.; Wu, L. M. *Langmuir* **2005,** *21,* 2124.

21. Ding, X.; Zhao, J.; Liu, Y.; Zhang, H.; Wang, Z. *Mater. Lett.* **2004,** *58,* 3126.

22. Wang, Y.; Ke, Y.; Li, J.; Du, S.; Xia, Y. *China Particuol.* **2007,** *5,* 300.

23. Bourgeat-Lami, E.; Lang, J. *J. Colloid Interface Sci.* **1998,** *197,* 293.

24. Bourgeat-Lami, E.; Lang, J. *J. Colloid Interface Sci.* **1999,** *210,* 281.

25. Huang, Z. B.; Tang, F. Q. *Acta Polym. Sin.* **2004,** *1,* 835.

26. Chen, C.-W.; Chen, C.-Y. *Colloid Polym. Sci.* **2009,** *287,* 1377.

27. Guo, L.; Pei, G.; Wang, T.; Wang, Z.; Jin, Y. *Colloids Surf. A Physicochem. Eng. Aspects* **2007,** *293,* 58.

28. Ragaert, K.; Dekeyser, A.; Cardon, L.; Degrieck, J. *J. Appl. Polym. Sci.* **2011,** *120,* 2872.

29. Signori, F.; Coltelli, M. B.; Bronco, S. *Polym. Degrad. Stabil.* **2009,** *94,* 74.

30. Bhattarai, N.; Jiang, W. Y.; Kim, H. Y.; Lee, D. R.; Park, S. J. *J. Polym. Sci. B Polym. Phys.* **2004,** *42,* 2558.

31. Salvo, P.; Raedt, R.; Carrette, E.; Schaubroeck, D.; Vanfleteren, J.; Cardon, L. *Sens. Actuat. A Phys.* **2012,** *174,* 96.

32. Arshady, R. *Colloid Polym. Sci.* **1992,** *270,* 717.

33. Chen, C.-W.; Chen, C.-Y.; Lin, C.-L. *J. Polym. Res.* **2011,** *18,* 587.

34. Fadda, S.; Cincotti, A.; Concas, A.; Pisu, M.; Cao, G. *Powder Technol.* **2009,** *194,* 207.

35. Deckers, J.; Shahzad, K.; Vleugels, J.; Kruth, J.-P. *Rapid Prototyping J.* **2012,** *18,* 409.

36. Kim, J.; Creasy, T. S. *Polym. Test.* **2004,** *23,* 629.

37. Drummer, D.; Rietzel, D.; Kühnlein, F. *Phys. Proc.* **2010,** *5,* 533.

38. Fox, T. G.; Flory, P. J. *J. Appl. Phys.* **1950,** *21,* 581.

39. Wunderlich, B. Thermal Analysis; Academic Press: New York, **1990.**

40. Andrews, R. J.; Grulke, E. A. In Polymer Handbook; Brandrup, J., Immergut, E. H., Eds.; Wiley: New York, **1999;** p VI212.

41. Haldorai, Y.; Lyoo, W. S.; Noh, S. K.; Shim, J.-J. *React. Funct. Polym.* **2010,** *70,* 393.

42. Rieger, J. *J. Therm. Anal.* **1996,** *46,* 965.

43. Deckers, J.; Kruth, J.-P.; Cardon, L.; Shahzad, K.; Vleugels, J. Proceedings of the 5th International PMI Conference **2012,** in press.

44. Liu, P.; Liu, W.-M.; Xue, Q.-J. *Des. Monomers Polym.* **2004,** *7,* 253.

45. Thomson, B.; Rudin, A.; Lajoie, G. *J. Appl. Polym. Sci.* **1996,** 59, 2009.